DØConference note 5144

Lifetime Difference and Mixing Phase in the B_s System

The DØ Collaboration
URL http://www-d0.fnal.gov
(Dated: July 24, 2006)

We present a study of the decay $B_s^0 \to J/\psi\phi$. From a simultaneous fit to the distributions in the candidate mass, proper decay length, and three angles of the decay products, we obtain the average lifetime of the (B_s^0, $\overline{B}_s^0$) system, $\overline{\tau}(B_s^0)$ =1.49 ±0.08 (stat)$^{+0.01}_{-0.03}$ (syst) ps, the width difference between the light and heavy mass eigenstates, $\Delta\Gamma \equiv (\Gamma_L - \Gamma_H)$ = 0.17 ± 0.09 ±0.03 ps^{-1}, and the CP-violating phase $\delta\phi$ = -0.79 ± 0.56 (stat) ± 0.01 (syst). Under the hypothesis of no CP violation ($\delta\phi \equiv 0$), we obtain $\overline{\tau}(B_s^0)$ =1.52 ±0.08$^{+0.01}_{-0.04}$ ps and $\Delta\Gamma = 0.12 \pm 0.08^{+0.03}_{-0.04}$ ps^{-1}. The data sample corresponds to an integrated luminosity of 1.0 fb^{-1} accumulated with the DØ detector at the Tevatron. All results are preliminary.

Preliminary Results for Summer 2006 Conferences

I. INTRODUCTION

In the standard model (SM), the light (L) and heavy (H) eigenstates of the B_s^0 system are expected to mix in such a way that the mass and decay width differences between them, $\Delta M \equiv M_H - M_L$ and $\Delta\Gamma \equiv \Gamma_L - \Gamma_H$, are sizeable. The mixing phase is predicted to be small, and to a good approximation the two mass eigenstates are expected to be CP eigenstates. New phenomena may introduce a non-vanishing mixing phase $\delta\phi$, leading to a reduction of the observed $\Delta\Gamma$ compared to the SM prediction [1] $\Delta\Gamma_{SM}$: $\Delta\Gamma = \Delta\Gamma_{SM} \times |(cos(\delta\phi)|$. While the mass difference has recently been measured with a high precision [2], the mixing phase has remained unknown.

The decay $B_s^0 \to J/\psi\phi$, proceeding through the quark process $b \to c\bar{c}s$, gives rise to both CP-even and CP-odd final states. It is possible to separate the two CP components of the decay $B_s^0 \to J/\psi\phi$, and thus to measure the lifetime difference, through a simultaneous study of the time evolution and angular distributions of the decay products of the J/ψ and ϕ mesons. Moreover, with a sizeable lifetime difference, there is a sensitivity to the mixing phase through the interference terms between the CP-even and CP-odd waves.

In Ref. [3] we presented an analysis of the decay chain $B_s^0 \to J/\psi\phi$, $J/\psi \to \mu^+\mu^-$, $\phi \to K^+K^-$ based on $\approx$450 pb^{-1} of data. In that analysis, we performed an unbinned maximum likelihood fit to the data, including the B_s candidate mass, lifetime, and the transversity polar angle. We extracted three parameters characterizing the B_s^0 system and its decay $B_s^0 \to J/\psi\phi$: $\overline{\tau} = 1/\overline{\Gamma}$, where $\overline{\Gamma} \equiv (\Gamma_H + \Gamma_L)/2$; $\Delta\Gamma/\overline{\Gamma}$; and the relative rate of the decay to the CP-odd states at time zero. Here we present new results, based on a two-fold increase in statistics. We extract $\overline{\tau}$, $\Delta\Gamma$, and the CP violating phase $\delta\phi$. We also measure the magnitudes of the decay amplitudes, and their relative phases.

II. DATA

The data were collected between June 2002 and January 2006. The preselected events include two reconstructed muons with a transverse momentum greater than 1.5 GeV. Each muon is required to be detected as a track segment in at least one layer of the muon system, and to be matched to a central track. One muon is required to have segments both inside and outside the toroid. We require the events to satisfy a muon trigger that does not include a cut on the impact parameter. The muon system covers the pseudorapidity range to $|\eta| \approx 2$. The sample corresponds to an integrated luminosity of 1 fb^{-1}.

To select the B_s^0 candidate sample, we apply the following kinematic and quality cuts. Minimum values of momenta in the transverse plane for B_s^0, ϕ, and K mesons are set at 6.0 GeV, 1.5 GeV, and 0.7 GeV, respectively. J/ψ candidates are accepted if the invariant mass is in the range 2.9 – 3.3 GeV. Successful candidates are constrained to the world average mass of the J/ψ meson [4]. Decay products of the ϕ candidates are required to satisfy a fit to a common vertex and to have an invariant mass in the range 1.01 – 1.03 GeV. We require the $(J/\psi, \phi)$ pair to be consistent with coming from a common vertex, and to have an invariant mass in the range 5.0 – 5.8 GeV. In case of multiple ϕ meson candidates, we select the one with the highest transverse momentum. Monte Carlo (MC) studies show that the p_T spectrum of the ϕ mesons coming from B_s^0 decay is harder than the spectrum of a pair of random tracks from hadronization. We define the signed decay length of a B_s^0 meson L_{xy}^B as the vector pointing from the primary vertex to the decay vertex projected on the B_s^0 transverse momentum. To reconstruct the primary vertex, we select tracks with $p_T > 0.3$ GeV that are not used as decay products of the B_s^0 candidate, and apply a constraint to the average beam spot position. The proper decay length, ct, is defined by the relation $ct = L_{xy}^B \cdot M_{B_s^0}/p_T$ where $M_{B_s^0}$ is the measured mass of the B_s^0 candidate. The distribution of the proper decay length uncertainty $\sigma(ct)$ of B_s^0 mesons peaks around 25 μm. We accept events with $\sigma(ct) < 60$ μm. There are 23343 events satisfying the above cuts.

III. FITTING PROCEDURE

We perform a simultaneous unbinned maximum likelihood fit to the proper decay length, three decay angles, and mass. The likelihood function $\mathcal{L}$ is given by:

$$\mathcal{L} = \prod_{i=1}^{N} [f_{sig}\mathcal{F}_{sig}^i + (1 - f_{sig})\mathcal{F}_{bck}^i], \tag{1}$$

where N is the total number of events, $\mathcal{F}_{sig}^i$ is a function of the signal mass, proper decay length, and the decay angles, $\mathcal{F}_{bck}^i$ is the product of the background mass, proper decay length, and angular density functions, and f_{sig} is the fraction of signal in the sample. Background is divided into two categories, based on their origin and lifetime characteristics. "Prompt" background is due to directly produced J/ψ mesons accompanied by random tracks arising

from hadronization. This background is distinguished from "non-prompt" background, where the J/ψ meson is a product of a B-hadron decay while the tracks forming the ϕ candidate emanate from a multibody decay of the same B hadron or from hadronization. We allow for independent parameters for the two background components in mass, lifetime, and decay angles.

Signal parametrization

The time evolution of the three-angle distribution of the products of the decay of *untagged* B_s^0 mesons, i.e., summed over B_s^0 and $\overline{B}_s^0$, expressed in terms of the linear polarization amplitudes $|A_x(t)|$ and their relative phases δ_i is [1]:

$$\frac{d^3\Gamma(t)}{d\cos\theta\ d\varphi\ d\cos\psi} \propto\ 2|A_0(0)|^2\ \mathcal{T}_+\ \cos^2\psi(1-\sin^2\theta\cos^2\varphi)$$

$$+\sin^2\psi\{|A_\parallel(0)|^2\ \mathcal{T}_+\ (1-\sin^2\theta\sin^2\varphi)+|A_\perp(0)|^2\ \mathcal{T}_-\ \sin^2\theta\}$$

$$+\frac{1}{\sqrt{2}}\sin 2\psi|A_0(0)||A_\parallel(0)|\cos(\delta_2-\delta_1)\ \mathcal{T}_+\ \sin^2\theta\sin 2\varphi$$

$$+\left\{\frac{1}{\sqrt{2}}|A_0(0)||A_\perp(0)|\cos\delta_2\sin 2\psi\sin 2\theta\cos\varphi\right.$$

$$\left.-|A_\parallel(0)||A_\perp(0)|\cos\delta_1\sin^2\psi\sin 2\theta\sin\varphi\right\}\frac{1}{2}\left(e^{-\Gamma_H t}-e^{-\Gamma_L t}\right)\sin(\delta\phi)\ . \tag{2}$$

where, $\mathcal{T}_+ = \frac{1}{2}\left((1+cos\delta\phi)e^{-\Gamma_L t}+(1-cos\delta\phi)e^{-\Gamma_H t}\right)$ and $\mathcal{T}_- = \frac{1}{2}\left((1-cos\delta\phi)e^{-\Gamma_L t}+(1+cos\delta\phi)e^{-\Gamma_H t}\right)$.

In the coordinate system of the J/ψ rest frame (where the ϕ meson moves in the x direction, the z axis is perpendicular to the decay plane of $\phi \to K^+K^-$, and $p_y(K^+) \geq 0$), the transversity polar and azimuthal angles (θ, φ) describe the direction of the μ^+, and ψ is the angle between $\vec{p}(K^+)$ and $-\vec{p}(J/\psi)$ in the ϕ rest frame. The quantity $\delta\phi$ is a CP-violating weak phase, due to the interference effects between $B_s^0 - \overline{B}_s^0$ mixing and decay processes.

We model the acceptance in the three angles by polynomials, with parameters determined using Monte Carlo simulations. We have used the *SVV_HELAMP* model in the EvtGen generator [5], interfaced to the Pythia program [6]. Simulated events were reweighted to match the kinematic distributions observed in the data.

Background parametrization

The lifetime shape of the background is described as a sum of a prompt component, simulated as a Gaussian function centered at zero, and a non-prompt component, simulated as a superposition of one exponential for the negative ct region and two exponentials for the positive ct region, with free slopes and normalization. The mass distributions of the backgrounds are parametrized by low-order polynomials: one- for the prompt component, two- for the non-prompt component). The distributions in the transversity polar angle of backgrounds are parametrized as $(1+X_{2x}\cos^2\theta+X_{4x}\cos^4\theta)$. The φ dependence of background is described by a function $1+Y_{1x}\cos(2\varphi)+Y_{2x}\cos^2(2\varphi)$. For the background dependence on the angle ψ, we use the function $1+Z_{2x}\cos^2(\psi)$. We also allow for a background term analogous to the interference term of the CP-even waves, with a free coefficient $intbkg_x$. As mentioned before, for each of the above background functions we use two separate sets of parameters for the prompt ($x = p$) and non-prompt ($x = l$) components. The 32 free parameters of the fit are listed in table I.

IV. RESULTS

Our results, and comparisons with previous measurements, are presented in Table II. The correlation matrix for the physics parameters is given in Table III. Results for the one standard deviation range for alternative fits, at discrete values of $\Delta\Gamma$ are shown in Table IV.

For the CP-violating phase, the fit returns the one standard deviation range $\delta\phi = -0.79 \pm 0.56$, consistent with the SM prediction of -0.03. The statistical uncertainty resulting from the fit is in agreement with the results of an ensemble test described later. (Note that there is an ambiguity inherent in this measurement. The distributions in the observables remain unchanged after a simultaneous flip of the signs of the sine and cosine of $\delta\phi$ and of $\Delta\Gamma$. Figures 2

	Parameter notation	description
1	f_{sig} (N_{sig})	fraction of the signal in the total number of candidate events ($N_{sig} = f_{sig} \times N_{tot}$).
2	M	The mean value of the Gaussian function in the signal mass PDF.
3	σ	The width of the Gaussian function in the signal mass PDF.
4	$\overline{\tau}$	The inverse of the average decay width, $\overline{\tau} = 1/\overline{\Gamma}$, where $\overline{\Gamma} = (\Gamma_L + \Gamma_H)/2$.
5	$\Delta\Gamma$	Decay width difference between two CP eigenstates of (B_s^0, $\overline{B}_s^0$) system, $\Delta\Gamma = \Gamma_L - \Gamma_H$.
6	$A_\perp(0)$	The magnitude of the CP-odd linear polarization amplitude at time t=0 in $B_s^0 \to J/\psi\phi$ decay. The fraction of CP-odd component at time t=0 is given by $R_\perp = \|A_\perp(0)\|^2$ and $(1 - R_\perp) = \|A_{\|\|}(0)\|^2 + \|A_0(0)\|^2$.
7	$\|A_0(0)\|^2 - \|A_{\|\|}(0)\|^2$	The difference of CP-even linear polarization amplitudes squared at time t=0 in $B_s^0 \to J/\psi\phi$ decay.
8	δ_1	$\equiv Arg(A_{\|\|}(0)^* A_\perp(0))$, $CP - conserving$ strong phase, expected to be mod π.
9	δ_2	$\equiv Arg(A_0(0)^* A_\perp(0))$, $CP - conserving$ strong phase, expected to be 0.
10	$\delta\phi$	$CP - violating$ weak phase. It can be expressed in terms of elements of the CKM matrix as $e^{i\delta\phi} = \frac{V_{ts}V_{tb}^*V_{cs}^*V_{cb}}{V_{ts}^*V_{tb}V_{cs}V_{cb}^*}$, expected to be very small $\mathcal{O}(0.03)$.
11	S	The scale factor for the the proper decay length uncertainty ($\sigma(ct)$).
12	a_{1p}	The coefficient of the mass term in the linear parametrization, describing the mass distribution of prompt background.
13	a_{1l}	The coefficient of the linear term in 2nd order polynomial $1 + a_{1l}m + a_{2l}m^2$, describing the mass distribution of non-prompt background.
14	a_{2l}	same as above but coefficient of the quadratic term.
15	f_-	The normalization constant of the exponential at $ct < 0$ in the background lifetime PDF.
16	f_+	The normalization constant of the first exponential at $ct > 0$ in the background lifetime PDF.
17	f_{++}	The normalization constant of the second exponential at $ct > 0$ in the background lifetime PDF.
18	b_-	The slope of the exponential function at $ct < 0$ in the background lifetime PDF.
19	b_+	The slope of the first exponential function at $ct > 0$ in the background lifetime PDF.
20	b_{++}	The slope of the second exponential function at $ct > 0$ in the background lifetime PDF.
21	X_{2p}	Coefficient of $cos^2\theta$ term in the polynomial $1 + X_{2p}cos^2\theta + X_{4p}cos^4\theta$, describing the transversity polar angle distribution of the prompt background.
22	X_{4p}	same as above but of $cos^4\theta$ term.
23	X_{2l}	Coefficient of $cos^2\theta$ term in the polynomial $1 + X_{2l}cos^2\theta + X_{4l}cos^4\theta$, describing the transversity polar angle distribution of the non-prompt background.
24	X_{4l}	same as above but of $cos^4\theta$ term.
25	Y_{1p}	Coefficient of $cos(2\phi)$ term in the polynomial $1 + Y_{1p}cos(2\phi) + Y_{2p}cos^2(2\phi)$, describing the ϕ-angle distribution of the prompt background.
26	Y_{2p}	same as above but of $cos^2(2\phi)$ term.
27	Y_{1l}	Coefficient of $cos(2\phi)$ term in the polynomial $1 + Y_{1l}cos(2\phi) + X_{2l}cos^2(2\phi)$, describing the ϕ-angle distribution of the non-prompt background.
28	Y_{2l}	same as above but of $cos^2(2\phi)$ term.
29	Z_{2p}	Coefficient of $cos^2\psi$ term in the polynomial $1 + Z_{2p}cos^2\psi$, describing the ψ-angle distribution of the prompt background.
30	Z_{2l}	Coefficient of $cos^2\psi$ term in the polynomial $1 + Z_{2l}cos^2\psi$, describing the ψ-angle distribution of the non-prompt background.
31	Int_p	Allowing for a term analogous to line 3 of Eq. 2 for the prompt background.
32	Int_l	Allowing for a term analogous to line 3 of Eq. 2 for the non-prompt background.

TABLE I: Definition of the fit parameters used in the unbinned maximum likelihood fit.

- 5 show the fit projections on the three decay angles and on the lifetime distribution. Figure 6 shows the 1-σ contour for $\Delta\Gamma$ versus c$\overline{\tau}$. Figure 7 shows the 1-σ contour for $\Delta\Gamma$ versus $\delta\phi$. The likelihood scan as a function of $\delta\phi$ is shown in Fig. 9.

We have explored the constraintt [8] on the CP-violating parameter from the recent preliminary DØ measurement of the charge asymmetry in muon pairs. The 1-σ contour for $\Delta\Gamma$ versus $\delta\phi$ for this fit is shown in Fig. 8. The results are listed in the Summary. Figure 11 illustrates the present status of the predicted and measured range of the B_s^0 mixing amplitude in the complex plane. We perform an alternative fit to the present data, under the hypothesis of

CP conservation, by setting $\delta\phi$ and δ_2 to zero and allowing δ_1 to vary. Results of this fit are shown in Table II in the column marked "$D\emptyset$ '06 CP conserved". The likelihood scan as a function of $\delta\phi$ is shown in Fig. 10.

To test the accuracy and statistical precision of the results, we perform 1000 pseudo-experiments with similar statistical sensitivity, generated with the same parameters as obtained in this analysis under the hypothesis of CP conservation. The pseudo-experiments are then analysed by the same fitting procedure as used for data: (1) assuming an arbitrary degree of CP violation, and (2) under the assumption of CP conservation. The results are shown in Figs. 14. and 13.

The pull distributions of parameters $\Delta\Gamma$ and $c\tau$ for the case of CP conservation are shown in Fig. 13. The fitted distributions are in agreement with the simulation. When the CP-violating angle is allowed to float, the correlation between the parameters $\Delta\Gamma$, c$\overline{\tau}$ and $\delta\phi$ results in the asymmetric distributions and tails in the distributions of statistical undertanities expected for experiments with ≈1000 signal events. We find ≈20% of experiments with the uncertanties equal or less than those obtained for data. For those experiments, the spread of the fitted values and their uncertainties for $\delta\phi$ are well described by the simulation, see the pull distribution in the fifth and sixth panels in Fig. 14. The fitted parameter $\Delta\Gamma$ for the case of free $\delta\phi$ is higher than the input value of 0.12 ps^{-1}. The difference is correlated with the fitted value of $\delta\phi$ as shown in Fig. 15.

TABLE II: Comparison of the existing direct measurements of decay rate difference between B_s^0 mass eigenstates ($\Delta\Gamma$), the average lifetime (i.e. inverse of the average decay rate, $\overline{\tau} = 1/\overline{\Gamma}$), the CP-violating weak phase ($\delta\phi$), and decay amplitudes to the $(J/\psi, \phi)$ final state. For the case of free $\delta\phi$, we encounter a sign ambiguity. Our measurement correlates the two solutions for $\delta\phi$ with the two signs of $\Delta\Gamma$: $\delta\phi$=-0.79±0.56 corresponds to $\Delta\Gamma$ >0, while $\delta\phi$ = 2.35±0.56 corresponds to $\Delta\Gamma$ <0.

Observable	CDF '04	DØ '06 CP conserved	DØ '06 free $\delta\phi$
$\Delta\Gamma$ (ps^{-1})	$0.47^{+0.19}_{-0.24} \pm 0.01$	$0.12^{+0.08}_{-0.10}{}^{+0.03}_{-0.04}$	$0.17^{+0.09}_{-0.09}$
$\frac{1}{\overline{\Gamma}} = \overline{\tau}$ (ps)	$1.40^{+0.15}_{-0.13}$	$1.52^{+0.08}_{-0.08}{}^{+0.01}_{-0.04}$	$1.49^{+0.08}_{-0.08}$
$\delta\phi$	$\equiv 0$	$\equiv 0$	-0.79±0.56
$\lvert A_0(0)\rvert^2 - \lvert A_{\parallel}(0)\rvert^2$	0.355 ± 0.067	0.38±0.05± 0.01	0.37±0.06
$A_{\perp}(0)$	0.35 ±0.10	0.45±0.05	0.46±0.06
$\delta_1 - \delta_1$	1.94±0.36	2.6±0.4	2.6±0.4
δ_1	–	–	3.3±1.1
δ_2	–	–	0.7±1.0

TABLE III: Correlation coefficients for physics parameters.

	$\overline{\tau}$	$\Delta\Gamma$	δ_1	δ_2	$\delta\phi$	$A_{\perp}(0)$	$\lvert A_0(0)\rvert^2 - \lvert A_{\parallel}(0)\rvert^2$
$\overline{\tau}$		-.188	-0.269	-0.269	0.727	-0.379	0.070
$\Delta\Gamma$			0.291	0.318	-0.172	-0.426	-0.016
δ_1				0.932	-0.347	0.047	-0.001
δ_2					-0.379	0.063	-0.116
$\delta\phi$						-0.421	0.148
$A_{\perp}(0)$							0.231

Systematic uncertainties

Systematic uncertainties come from several sources. To test the sensitivity to the detection acceptance, we vary the parameters describing the efficiency by $\pm 1\sigma$. We also perform maximum likelihood fits using several alternative approaches to the function needed to match the kinematic distributions of simulated events and data. We use our earlier estimates [3] of the MC verification of the event processing and fitting procedure. The event processing and selection data entails additional uncertainties, not fully accounted for by MC simulations. About half of our present data sample was processed twice, with two different versions of the reconstruction program. The uncertainly also

TABLE IV: Fit results for $\delta\phi$ at fixed values of $\Delta\Gamma$.

$\Delta\Gamma$ (ps^{-1})	$\delta\phi$	$\Delta\ln(\mathcal{L})$
0.03	-0.84 ± 1.24	1.28
0.04	-0.83 ± 1.07	1.11
0.05	-0.82 ± 0.96	0.90
0.07	-0.81 ± 0.81	0.67
0.10	-0.79 ± 0.67	0.33
0.15	-0.778 ± 0.57	0.03
0.17	-0.785 ± 0.56	0.0
0.20	-0.81 ± 0.55	0.04

includes the effects of the variation of the B_s mass range, and other event selection thresholds. We use the difference of the fit results for the corresponding samples to set the uncertainty due to the inadequacies of the event processing. We use our earlier estimate of the effect of the imperfect detector alignement.

Our adopted definition of the measured proper decay time uses the measured mass of the canditate (J/ψ,ϕ) pair. Alternatively, one could use the world average B_s^0 mass. The difference in the decay length value changes the background lifetime parameters, but has little effect on the physics observables. We include the difference in the fit results for the two definitions in the discussion of the systematic uncertainties.

TABLE V: Sources of systematic uncertainty. The numbers reflect the variation of the fitted central values associated with the one-σ variation of the corresponding external input parameters.

Source	$c\tau(B_s^0)$ μm	$\Delta\Gamma$ ps^{-1}	$R_\perp$	$\lvert A_0(0)\rvert^2 - \lvert A_\parallel(0)\rvert^2$	δ_1	$\delta\phi$
Acceptance vs. θ,φ, ψ	$\pm$0.5	$\pm$0.001	$\pm$0.003	$\pm$0.01	$\pm$0.02	$\pm$0.01
Procedure test	$\pm$2.0	$\pm$0.025	$\pm$0.01	–	–	–
Event processing	$-$8.0	0.00	-0.01	–	–	–
Detector alignment	$\pm$2.0	–	–	–	–	–
ct definition	1.3	0.001	-0.001	-0.002	-0.009	-0.01
Total	$-$8.5,+3.2	$\pm$0.03	$\pm$0.01	$\pm$0.01	$\pm$0.02	$\pm$0.01

V. SUMMARY

From a fit to the time-dependent angular distribution of the untagged decays $B_s^0 \to J/\psi\phi$, we have measured the average lifetime of the (B_s^0, $\overline{B}_s^0$) system, $\overline{\tau}(B_s^0) = 1/\overline{\Gamma}$, and the width difference, $\Delta\Gamma$, between the light and heavy B_s^0 eigenstates, and the CP-violating phase. We also measured the magnitude of the decay amplitudes and the relative phase between A_0 and $A_\parallel$. We obtain:

$$\overline{\tau}(B_s^0) = 1.49 \pm 0.08^{+0.01}_{-0.03} \text{ ps}$$
$$\Delta\Gamma = 0.17 \pm 0.09 \pm 0.03 \text{ ps}^{-1}$$
$$\delta\phi = -0.79 \pm 0.56 \pm 0.01$$

Applying an additional constraint from the DØ preliminary measurement of the charge asymmetry in the B_s^0 decay, we obtain

$$\overline{\tau}(B_s^0) = 1.50 \pm 0.07^{+0.01}_{-0.03} \text{ ps}$$
$$\Delta\Gamma = 0.15 \pm 0.08 \pm 0.03 \text{ ps}^{-1}$$
$$\delta\phi = -0.56 \pm 0.40 \pm 0.01$$

$$R_\perp = |A_\perp(0)|^2 = 0.21 \pm 0.05 \pm 0.01$$
$$|A_0(0)|^2 - |A_\parallel(0)|^2 = 0.37 \pm 0.06 \pm 0.01$$
$$\delta_1 = 3.3 \pm 1.0 \pm 0.02$$
$$\delta_2 = 0.7 \pm 1.1 \pm 0.02$$

Note that our measurement does not resolve the sign ambiguity of $\Delta\Gamma$. It correlates the two solutions for $\delta\phi$ with the two signs of $\Delta\Gamma$: $\delta\phi$=-0.79$\pm$0.56 corresponds to $\Delta\Gamma > 0$, while $\delta\phi$ = 2.35$\pm$0.56 corresponds to $\Delta\Gamma < 0$.

Under the hypothesis of no CP violation ($\delta\phi = 0$), we obtain:

$$\overline{\tau}(B_s^0) = 1.52 \pm 0.08^{+0.01}_{-0.03} \text{ ps}$$
$$\Delta\Gamma = 0.12 \pm 0.08 \pm 0.03 \text{ ps}^{-1}$$

$$R_\perp = |A_\perp(0)|^2 = 0.21 \pm 0.05 \pm 0.01$$
$$|A_0(0)|^2 - |A_\parallel(0)|^2 = 0.37 \pm 0.06 \pm 0.01$$
$$\delta_1 - \delta_2 = 2.6 \pm 0.4 \pm 0.02$$

---

[1] I. Dunietz, R. Fleischer, and U. Nierste, hep-ph/0012219.
[2] CDF Collaboration, hep-ex/0606027.
[3] DØ Collaboration, V. M. Abazov *et al.*, Phys. Rev. Lett. **95**, 171801 (2005).
[4] S. Eidelman *et al.* (Particle Data Group), Phys. Lett. B **592**, 1 (2004) and 2005 partial update for edition 2006; http://pdg.lbl.gov 2005.
[5] A. Ryd, D. Lange, http://www.slac.stanford.edu/ lange/EvtGen/
[6] H. U. Bengtsson and T. Sjostrand, Comp. Phys. Comm. **46**, 43 (1987).
[7] Y. Grossman, Y. Nir, G. Raz, hep-ph/0605028v2.
[8] The relation between $\Delta\Gamma$, $\delta\phi$, and the charge asymmetry in the flavor-specific decays is $A_{sl} = \Delta\Gamma/\Delta M \times tan(\delta\phi)$, see U. Nierste, hep-ph/0406300. With $\Delta M = 17.3$ GeV, and $A_{sl} = -0.6 \pm 9.0) \times 10^{-3}$ (DØ note 5189-conf), we have $\Delta\Gamma \times tan((\delta\phi) = -0.01 \pm 0.156$.
[9] CDF Collaboration, D. Acosta *et al.*, Phys. Rev. Lett., **94**, 101803 (2005).
[10] CDF $B_s \to K^+K^-$ Conference note.
[11] DØ $B_s \to D_s^{(*)}D_s^{(*)}$ Conference note.
[12] M. Beneke, G. Buchalla, C. Greub, A. Lenz and U. Nierste, "Next-to-leading order QCD corrections to the lifetime difference of B/s mesons," Phys. Lett. B **459** (1999) 631 [arXiv:hep-ph/9808385]; input parameters updated in March 2006.

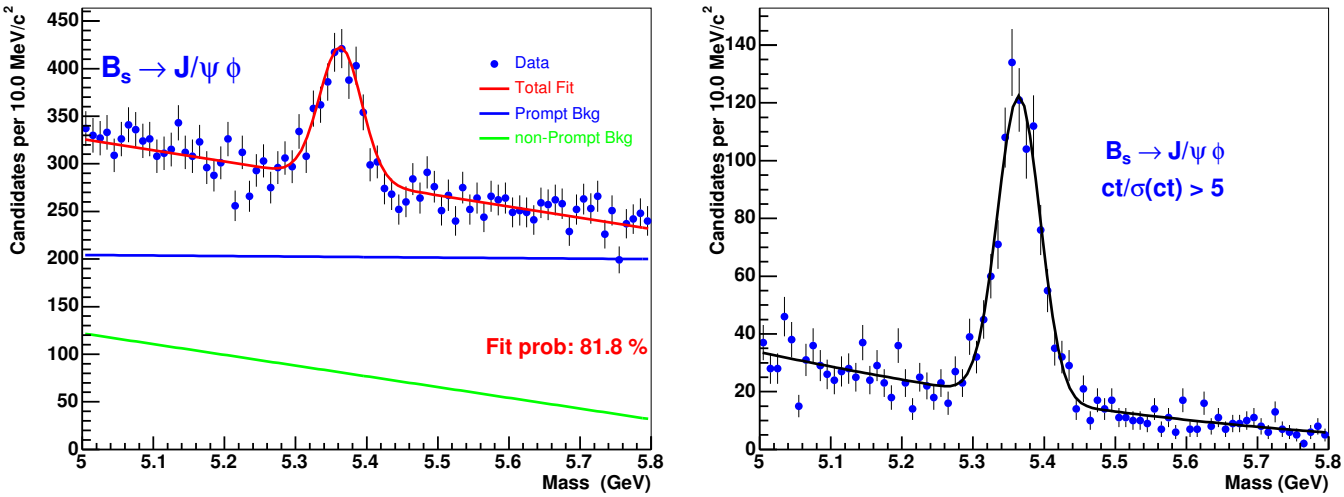

FIG. 1: The invariant mass distribution of the $(J/\psi, \phi)$ system for B_s^0 candidates. Left: All events. The curves are the projections of the maximum likelihood fit: prompt and non-prompt background and total. Right: Subsample with the prompt background suppressed. The curve is a fit to a Gaussian distribution and a linear background.

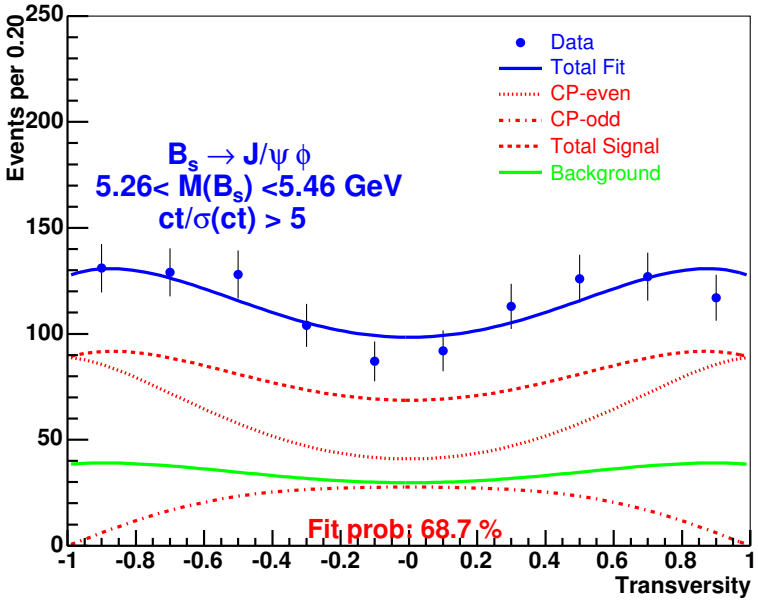

FIG. 2: The transversity polar angle distribution for the signal-enhanced subsample: "non-prompt" and signal mass range. The curves show: the signal contribution, dotted(red); the background, light solid (green); and total, solid(blue).

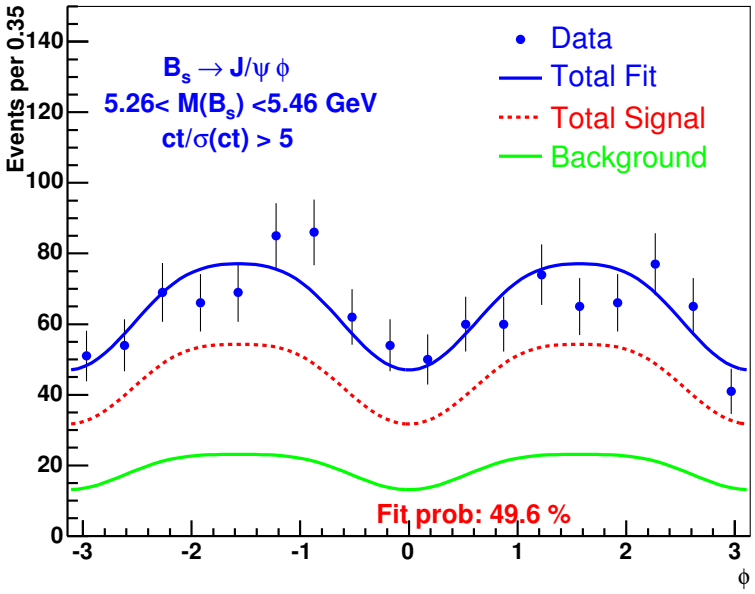

FIG. 3: The distribution in the transversity asimuthal angle φ for the signal-enhanced subsample: "non-prompt" and signal mass range. The curves show: the signal contribution, dotted(red); the background, light solid (green); and total, solid(blue).

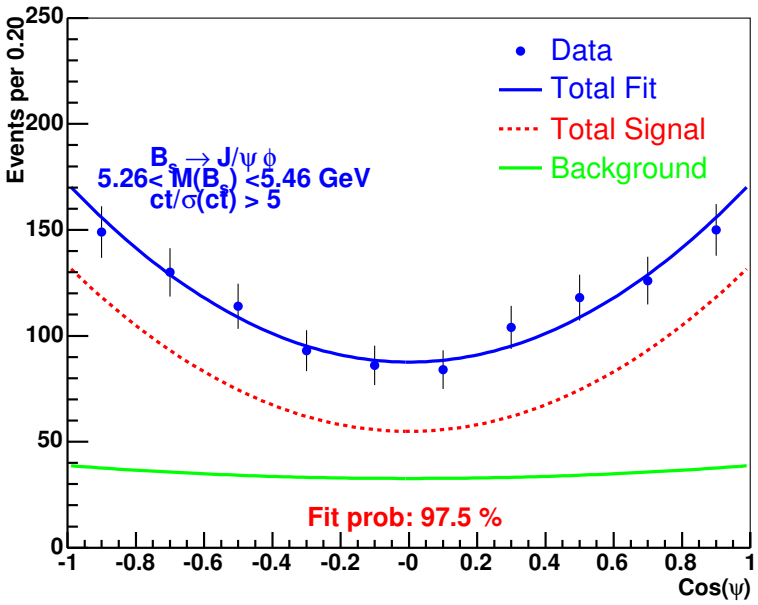

FIG. 4: The distribution in the angle ψ for the signal-enhanced subsample: "non-prompt" and signal mass range. The curves show: the signal contribution, dotted(red); the background, light solid (green); and total, solid(blue).

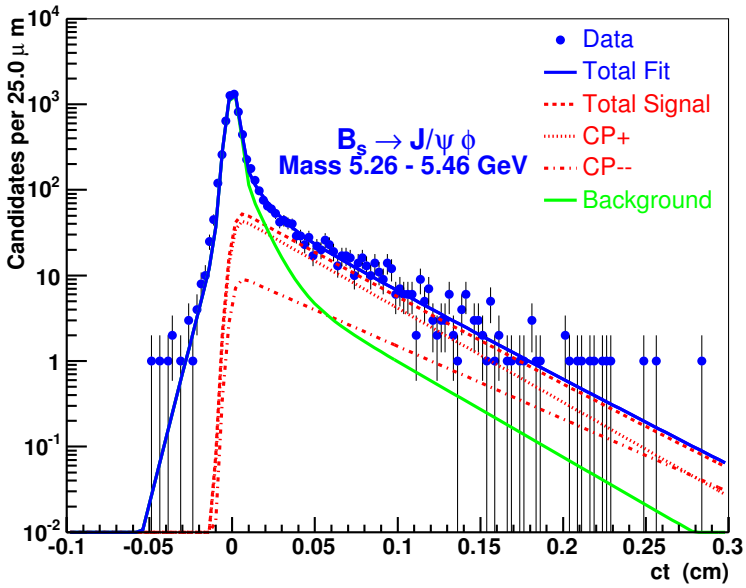

FIG. 5: The proper decay length, ct, of the B_s^0 candidates in the signal mass region. The curves show: the signal contribution, dashed(red); the CP-even (dotted) and CP-odd (dashed-dotted) contributions of the signal, the background, light solid(green); and total, solid(blue).

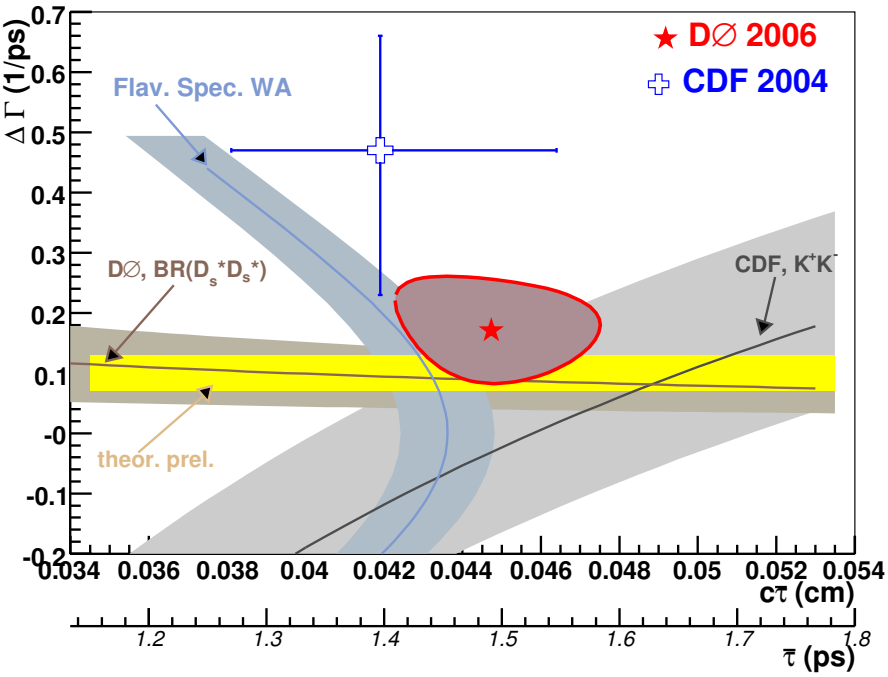

FIG. 6: The DØ one-σ (stat.) contour ($\delta \ln(L) = 0.5$) in the plane $\Delta\Gamma$ vs $c\overline{\tau}$, for the fit allowing an arbitrary degree of CP violation in the B_s^0 system. It is compared to a one-σ band for the world average [4] (WA) measurement based on flavor-specific decays, $\tau_{fs} = 1.454 \pm 0.040$ ps. Also shown is the CDF '2004 result [9], obtained under the assumption of CP conservation, the recent CDF measurement of the B_s^0 lifetime from the $B_s^0 \to K^+K^-$ decay [10], and the implication of the preliminary DØ result [11] of the branching fraction for the decay BR($B_s^0 \to D_s^* D_s^*$). The SM theoretical prediction [12] is shown as the horizontal band.

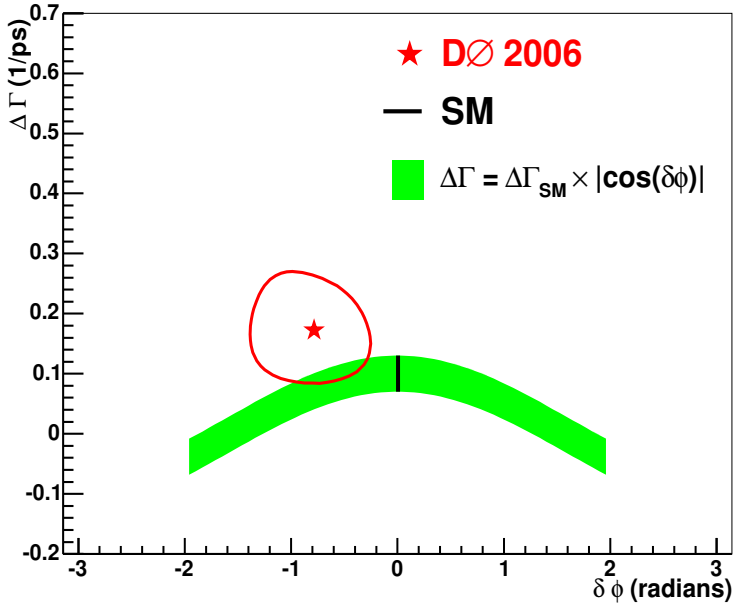

FIG. 7: The DØ one-σ (stat.) contour ($\delta \ln(L) = 0.5$) in the plane $\Delta\Gamma$ vs $\delta\phi$. Also shown is the one-σ band representing the theoretical prediction: $\Delta\Gamma = \Delta\Gamma_{SM} \times |(cos(\delta\phi)|$, with $\Delta\Gamma_{SM} = 0.10 \pm 0.03$ ps^{-1}.

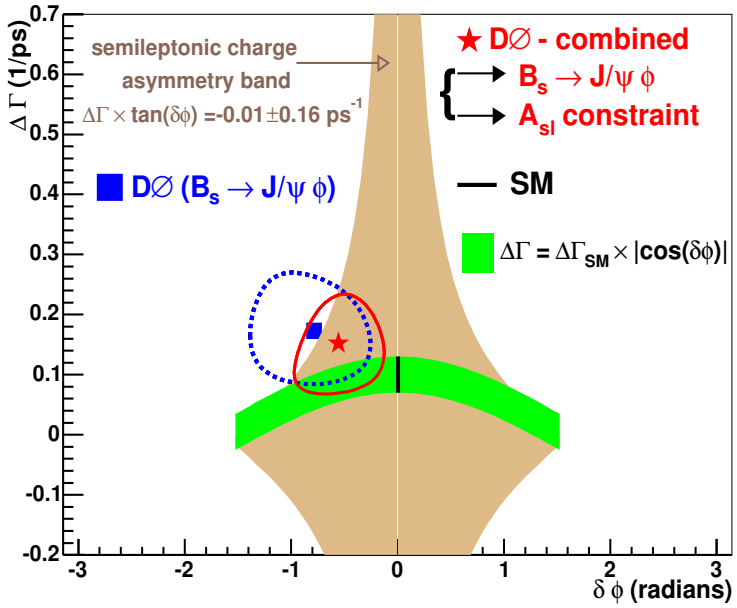

FIG. 8: The DØ one-σ (stat.) contour ($\delta \ln(L) = 0.5$) in the plane $\Delta\Gamma$ vs $\delta\phi$, for a fit including the constraint from the new DØ measurement of the charge asymmetry in semineptonic B_s^0 decay. Also shown is the one-σ band representing the theoretical prediction: $\Delta\Gamma = \Delta\Gamma_{SM} \times |(cos(\delta\phi)|$, with $\Delta\Gamma_{SM} = 0.10 \pm 0.03$ ps^{-1}.

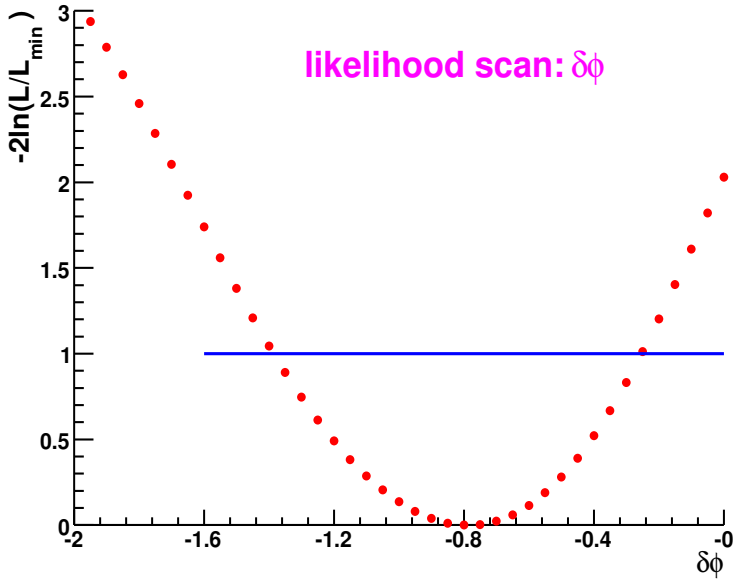

FIG. 9: The likelihood scan vs $\delta\phi$ for the default fit.

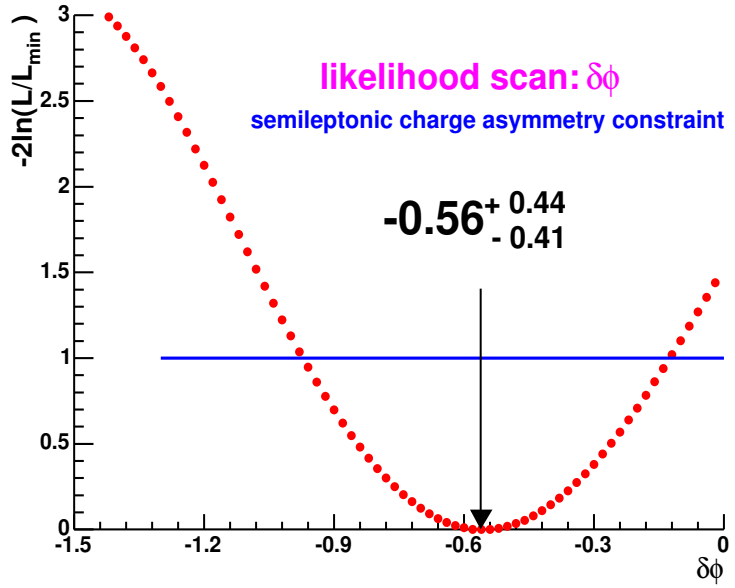

FIG. 10: The likelihood scan vs $\delta\phi$ for the fit including the constraint from the charge asymmetry in semileptonic decays.

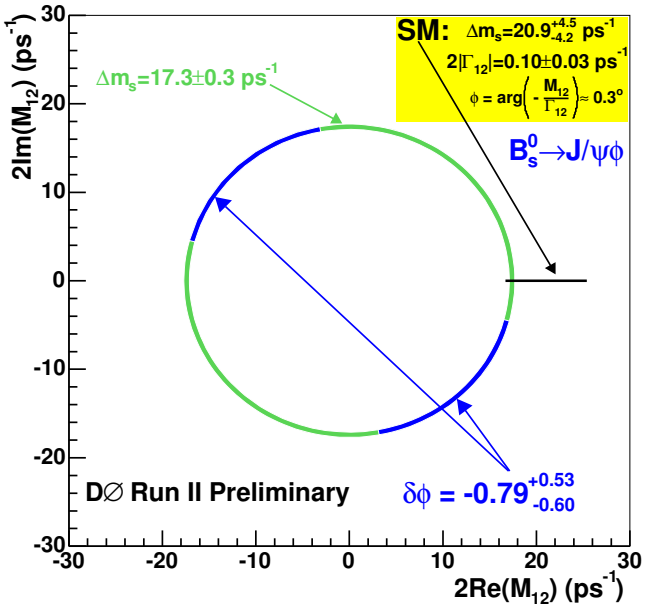

FIG. 11: The constraints on the B_s mixing amplitude in the complex plane. The green circle corresponds to the measured value of the mass difference. The direct measurement of mixing phase $\delta\phi$ is marked with blue.

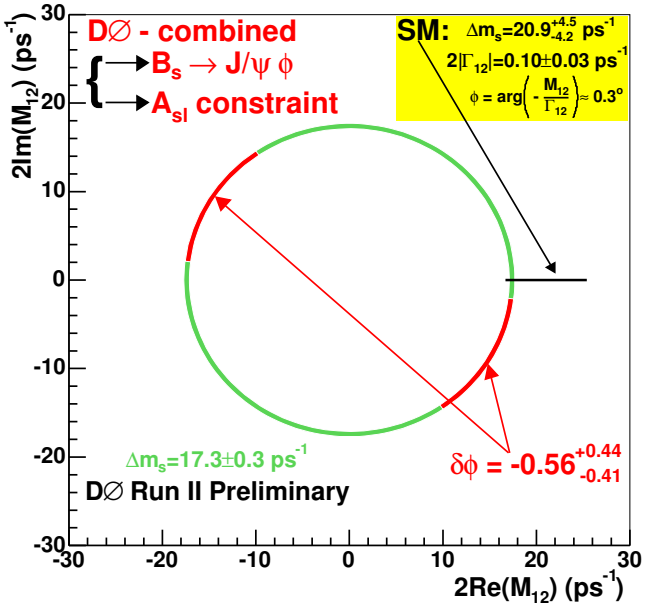

FIG. 12: The experimental constraints on the B_s mixing amplitude in the complex plane. The green circle corresponds to the measured value of the mass difference. The combined result of the direct measurement of mixing phase $\delta\phi$ from this study and from the DØ measurement of the charge asymmetry in semileptonic decays is marked with red.

FIG. 13: Pull distributions of the parameters $\Delta\Gamma$ and $c\overline{\tau}$, returned by fits to an ensemble of 1000 simulated experiments, assuming CP conservation.

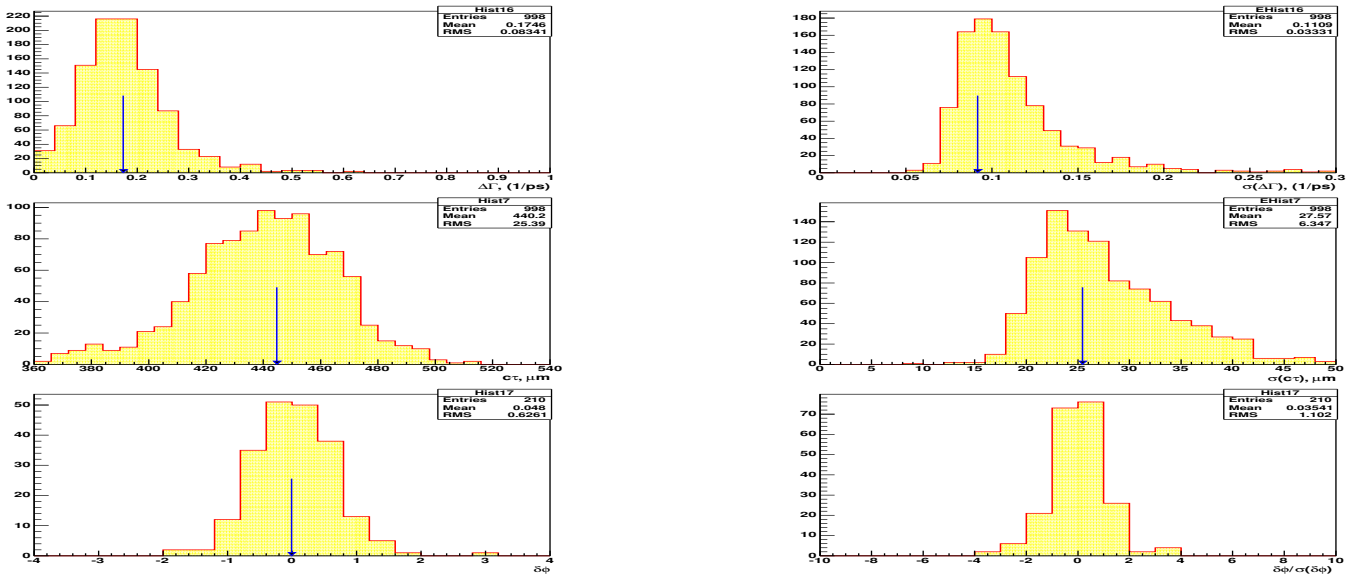

FIG. 14: Distribution of values and errors of the parameters $\Delta\Gamma$ (Top), and $c\tau$ (Middle), returned by fits to an ensemble of 1000 experiments simulated under the assumption of CP consservation. The fits allow an arbitrary degree of the CP violation. The fitted values of the parameters, and the statatistical uncertainties from the fit to DØ data are indicated by the arrows. The bottom panels show the distribution of $\delta\phi$ (the input is equal to zero, the DØ value is -0.78), and the corresponding pull for experiments with the statistical uncertainties of $\Delta\Gamma$ and $c\overline{\tau}$ equal or better than those obtained for data.

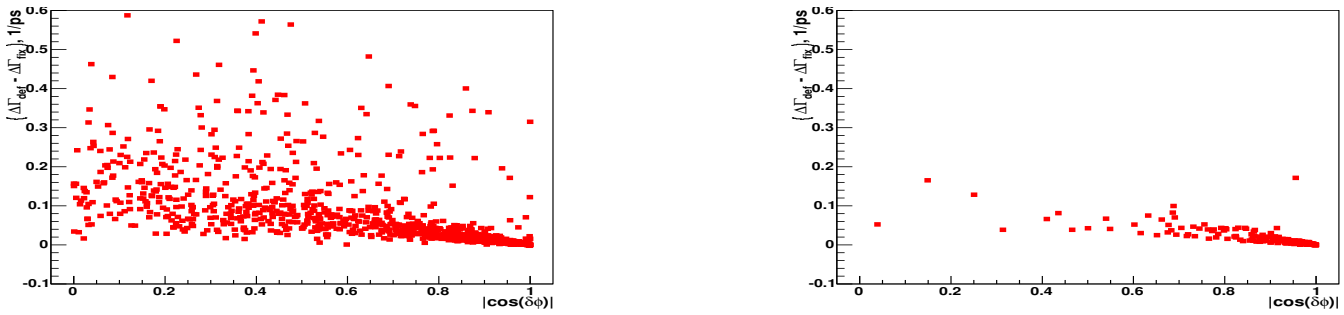

FIG. 15: Left:Scatter plot $\Delta\Gamma$ vs $|cos(\delta\phi)|$ for fits with a free $\delta\phi$ performed on the ensemble of 1000 pseudo-experiments generated with an assumption of $\delta\phi$=0. Right: the same for the subset of 210 experiments with statistical uncertainties of $\Delta\Gamma$ and $c\overline{\tau}$ equal or smaller than those obtained for data.